Supplementary Figure S1

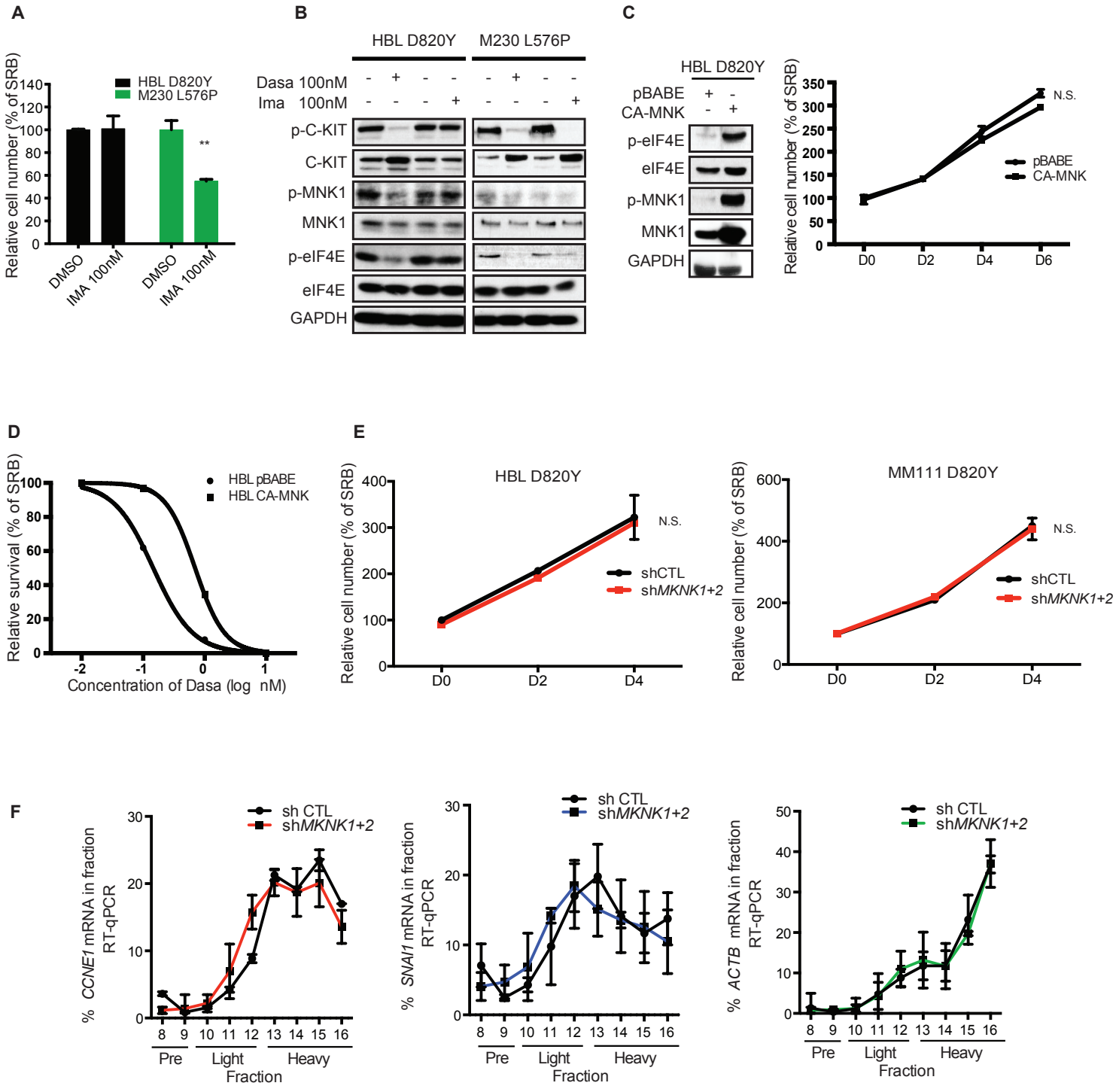

Supplementary Figure S1. Differential response to C-KIT inhibitor dasatinib and imatinib in HBL and M230 cells, and growth curves of HBL or MM111 cells with either CA-MNK overexpression or MNK1/2 depletion.
(A) Cell proliferation assessed by SRB staining 72 hours after treatment with vehicle (DMSO) or 100nM imatinib in HBL and M230. Data represent the mean ± SD, n=3. ** p<0.01, by Two-way ANOVA. (B) Western blot analysis of phospho-C-KIT, C-KIT, phospho-MNK1, MNK1, phospho-eIF4E, eIF4E and GAPDH in HBL and M230 cells treated with dasatinib or imatinib for 24 hours. (C) Western blot analysis of phospho-MNK1, MNK1, phospho-eIF4E, eIF4E and GAPDH in HBL pBABE and CA-MNK cell lines (left). Cell proliferation of HBL pBABE and CA-MNK cells, assessed by SRB staining (right). Data represent the mean ± SD, n=3. p>0.05, by Two-way ANOVA. (D) Cell proliferation assessed by SRB staining at 72 hours with vehicle (DMSO) or 0.1, 1, and 10nM dasatinib in HBL pBABE and CA-MNK cells. IC50 was determined using Prism version 4.0 (GraphPad Software, San Diego, CA). (E) Cell proliferation assessed by SRB staining in HBL and MM111 shCTL and sh*MKNK1+2* cells (96 hours) Data represent the mean ± SD, n=3. p>0.05, by Two-way ANOVA. (F) RT–qPCR to determine the distribution of *ACTB*, *SNAI1* and *CCNE1* mRNAs in polysome fractions. Data represent the mean ± SD, n=3.

Supplementary Figure S2

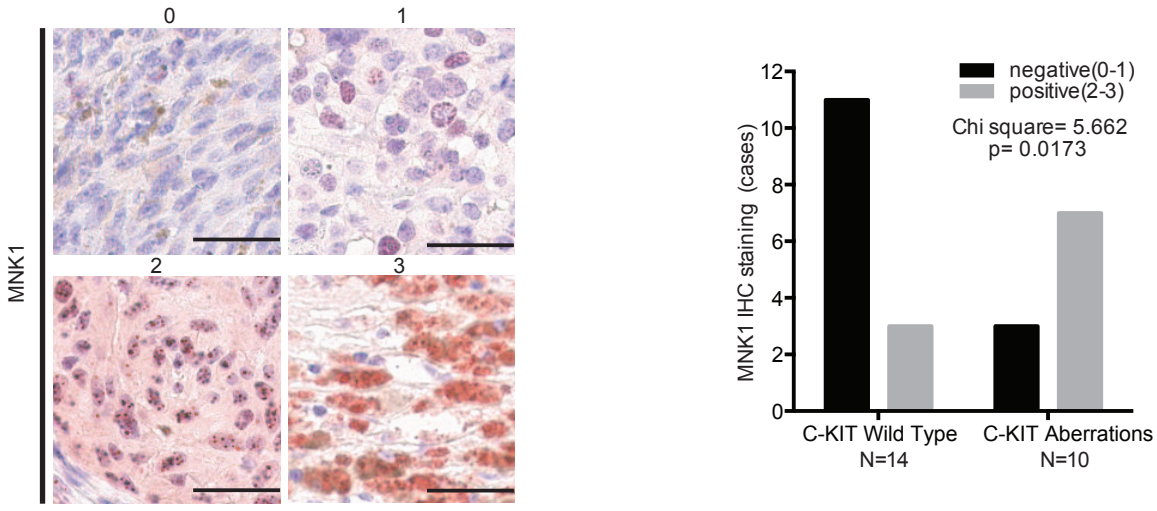

Supplementary Figure S2. MNK1 expression detected by IHC in C-KIT wild-type or mutant patient samples.
Representative images of MNK1 IHC staining are shown in the left panel. Bar graph of MNK1 IHC scores in melanoma patients is shown in the right panel. Chi-squared test, p values shown in the figure. For upper panels, scale bars: 200 μm, original magnification: x4. For lower panels, scale bars: 40 μm, original magnification: x20.

Supplementary Figure S3 Chemical synthesis of SLV-2436

A structure-driven approach was used to identify a novel class of amino-1*H*-indazol-1,2-dihydropyridin-2-one derivative as a potent MNK1/2 inhibitor. 5-(3-Amino-1*H*-indazol-6-yl)-1-[(3-chlorophenyl)methyl]-1,2-dihydropyridin-2-one **(1)** was synthesized in three steps, starting from a commercially available compound, 5-bromopyridin-2-ol **(2),** as shown in the scheme below. Nucleophilic substitution of pyridinone (**2)** reacted with 3-chlorobenzyl bromide resulting in an intermediate (**3),** which was subsequently used for the Miyaura borylation reaction to synthesize the boronate ester (**4**). The obtained boronate (**4)** and 6-bromo-1*H*-indazol-3-amine **(5)** served as coupling partners in the final Suzuki reaction, in which the final compound **SEL201-88** was synthesized with an overall yield of 49% allowing for multigram scale synthesis.

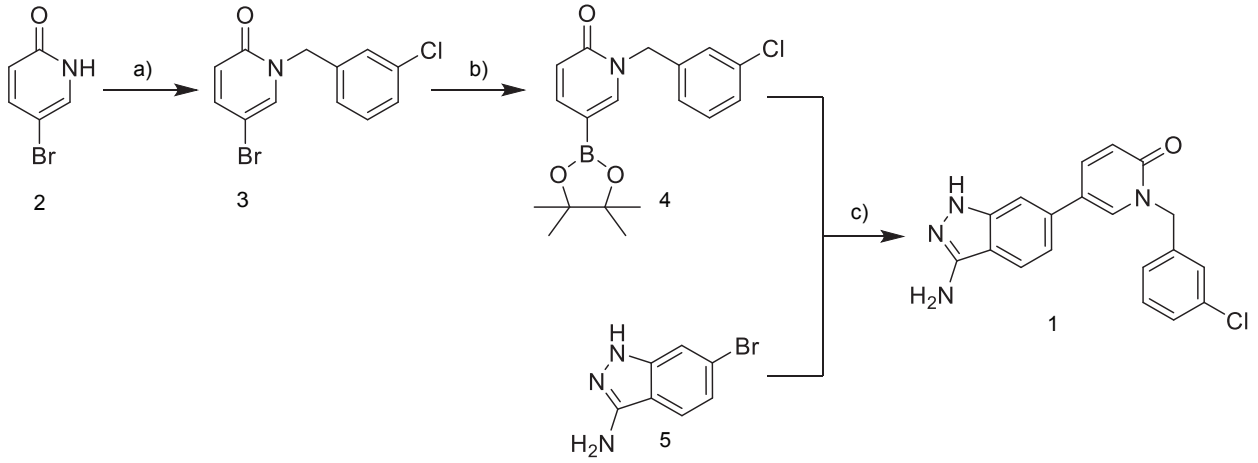

Reaction conditions: a) NaH 60% in oil (1.1eq), 3-chlorobenzyl bromide (1.1eq), DMF; b) Bis(pinacolato)diboron (1eq), CH_3COOK (3eq), $Pd(OAc)_2$ (0.1eq), Xphos (0.15eq), 1,4-dioxane; c) K_2CO_3 (2eq), $Pd(dppf)_2Cl_2$*DCM (0.03eq), 1,4-dioxane/water (2/1);

I. Experimental Procedures and Spectroscopic Data for Compounds.

General Procedures. All chemicals were purchased with the highest commercial quality and used without further purification, unless otherwise stated. Reactions were monitored through thin-layer chromatography (TLC) using Sigma Aldrich silica gel plates (60 F254) with UV light as the visualizing agent. Sigma Aldrich silica gel 63-200 mesh size was used for column chromatography. Melting points were obtained using a BUCHI Melting Point M-560 instrument. ^{1}H (400MHz), ^{13}C (101MHz) nuclear magnetic resonance spectra were recorded at ambient temperature with Varian Mercury – VX. Chemical shifts (δ) were reported in parts per million (ppm) and coupling constants (*J*) were given in hertz (Hz). The following abbreviations were used to explain the multiplicities: s=singlet, d=doublet, dd=doublet of doublets, m=multiplet. LC-MS analyses were performed on Bruker Amazon SL. Analytical separation was carried out on Waters Symmetry column C18 3.9x150mm 5µm with a flow rate of 1.2ml/min and detection at 254nm. The mobile phase composed of water (solvent A) and acetonitrile (solvent B), both containing 0.1% formic acid. HRMS analysis was performed on a Q Exactive™ Focus Hybrid Quadrupole-Orbitrap™ Mass Spectrometer. Yields refer to chromatographically and spectroscopically pure compounds unless otherwise stated.

Chemical synthesis and characterization of SEL201-88.

5-bromo-1-(3-chlorobenzyl)pyridin-2(1H)-one (**3**). The suspension of 5-bromopyridin-2-ol (5g, 28.7mmol) in dry DMF (50ml) was cooled to 0^{0}C, and then sodium hydride (60% in oil) (1.3g, 31.6mmol) was added in portions. The reaction mixture was stirred for 1h and then 3-chlorobenzyl bromide (4.2ml, 31.6mmol) was dropped into the reaction. After being stirred at room temperature overnight, the reaction was diluted with water and ethyl acetate. The layers were separated, and the aqueous layer was further extracted with ethyl acetate (3x). The organic layers were combined, washed with brine (2x), dried over Na_2SO_4, and further concentrated. The crude product was purified by column chromatography on silica gel (dichlorometane/methanol 9:1) to give 5-bromo-1-(3-chlorobenzyl)pyridin-2(1*H*)-one as a beige solid (6.6g, 77% yield). LC-MS (*m/z*) 266.7 $(M+H)^+$; HPLC purity 99%, t_R=2.9min; ^{1}H NMR (400MHz, DMSO-d_6) δ 8.22 (d, J=2.7 Hz, 1H), 7.56 (dd, J=9.7, 2.8 Hz, 1H), 7.47-7.34 (m, 3H), 7.34-7.25 (m, 1H), 6.43 (d, J=9.7Hz, 1H), 5.06 (s, 2H). ^{13}C NMR (101MHz, DMSO-d_6) δ 160.43, 143.36, 139.76, 139.40, 133.57, 130.98, 128.21, 128.14, 126.97, 121.94, 97.31, 51.44, 40.03; mp 89-90^o

1-[(3-chlorophenyl)methyl]-5-(tetramethyl-1,3,2-dioxaborolan-2-yl)-1,2-dihydropyridin-2-one (**4**). A mixture of 5-bromo-1-(3-chlorobenzyl)pyridin-2(1*H*)-one (**3**) (1.4g, 4.5mmol), bis(pinacolato)diboron (1.16g, 4.5mmol), potassium acetate (1.3g, 13.7mmol), X-Phos (0.32g, 0.68mmol) in dry 1,4-dioxane (15ml) were placed in a sealed tube under argon purge. The reaction mixture was degassed for further 10 min under a slow stream of argon before palladium(II) acetate (0.3g, 1.4mM) was added. The reaction mixture was heated to 80^{o}C and remained at this temperature for 30 min. After the reaction mixture was cooled to room temperature, it was subsequently filtered through Celite, washed with ethyl acetate and concentrated. Crude product was filtered by flash chromatography on silica gel (hexane/ethyl acetate 1:1) to obtain a mixture of 1-[(3-chlorophenyl)methyl]-5-(tetramethyl-1,3,2-dioxaborolan-2-yl)-1,2-dihydropyridin-2-one LC-MS (*m/z*) 263.9 $(M+1)^+$ and {1-[(3-chlorophenyl)methyl]-6-oxo-1,6-dihydropyridin-3-yl}boronic acid LC-MS (*m/z*) 346.0 $(M+1)^+$ as a dark yellow oil which was used for the next step of synthesis without further purification; yield 82%.

5-(3-amino-1H-indazol-6-yl)-1-[(3-chlorophenyl)methyl]-1,2-dihydropyridin-2-one (**1**). A mixture of 1-[(2-fluorophenyl)methyl]-5-(tetramethyl-1,3,2-dioxaborolan-2-yl)-1,2-dihydropyridin-2-one (1.48g, 4.3mmol), 6-bromo-1*H*-indazol-3-amine (0.65g, 3.1mmol), potassium carbonate (0.9g, 6mmol) in dioxane/water (2:1) were purged with argon for 10 minutes and then [1,1'-bis(diphenylphosphino)ferrocene]palladium(II) chloride, complex with dichloromethane (0.07g, 0.09mM) was added. The reaction mixture was heated to 120^{o}C and remained at this temperature under microwave irradiation for 30min. The reaction mixture was then cooled to room temperature, filtered through Celite and concentrated. The residue was purified by flash chromatography on silica (dichloromethane/methanol 95:5) to obtain the product, 5-(3-amino-1*H*-indazol-6-yl)-1-(2-fluorobenzyl)pyridin-2(1*H*)-one (0.6g, 78% yield), as a grey solid. LC-MS (*m/z*) 266.7 $(M+H)^+$; HPLC purity 100%, t_R=7.1min; ^{1}H NMR (400MHz, DMSO-d_6) δ 11.45 (s, 1H), 8.32 (d, J=2.5Hz, 1H), 7.90 (dd, J=9.5, 2.7Hz, 1H), 7.73 (d, J=8.4Hz, 1H), 7.47 (s, 1H), 7.13 (dd, J=8.4, 1.3Hz, 1H), 6.55 (d, J=9.5Hz, 1H), 5.36 (s, 2H), 5.20 (s, 2H). ^{13}C NMR (101MHz, DMSO-d_6) δ 161.14, 149.59, 142.47, 140.31, 140.27, 136.97, 134.36, 133.53, 130.94, 128.19, 127.99, 126.98, 121.31, 120.39, 119.68, 116.33, 113.59, 106.14, 51.65; HRMS *m/z* $[M+1]^+$ calcd for $C_{19}H_{15}ClN_4O$ 351,1007, found 351,1007.

Supplementary Figure S4 Pharmacodynamics and pharmacokinetic properties of SEL201

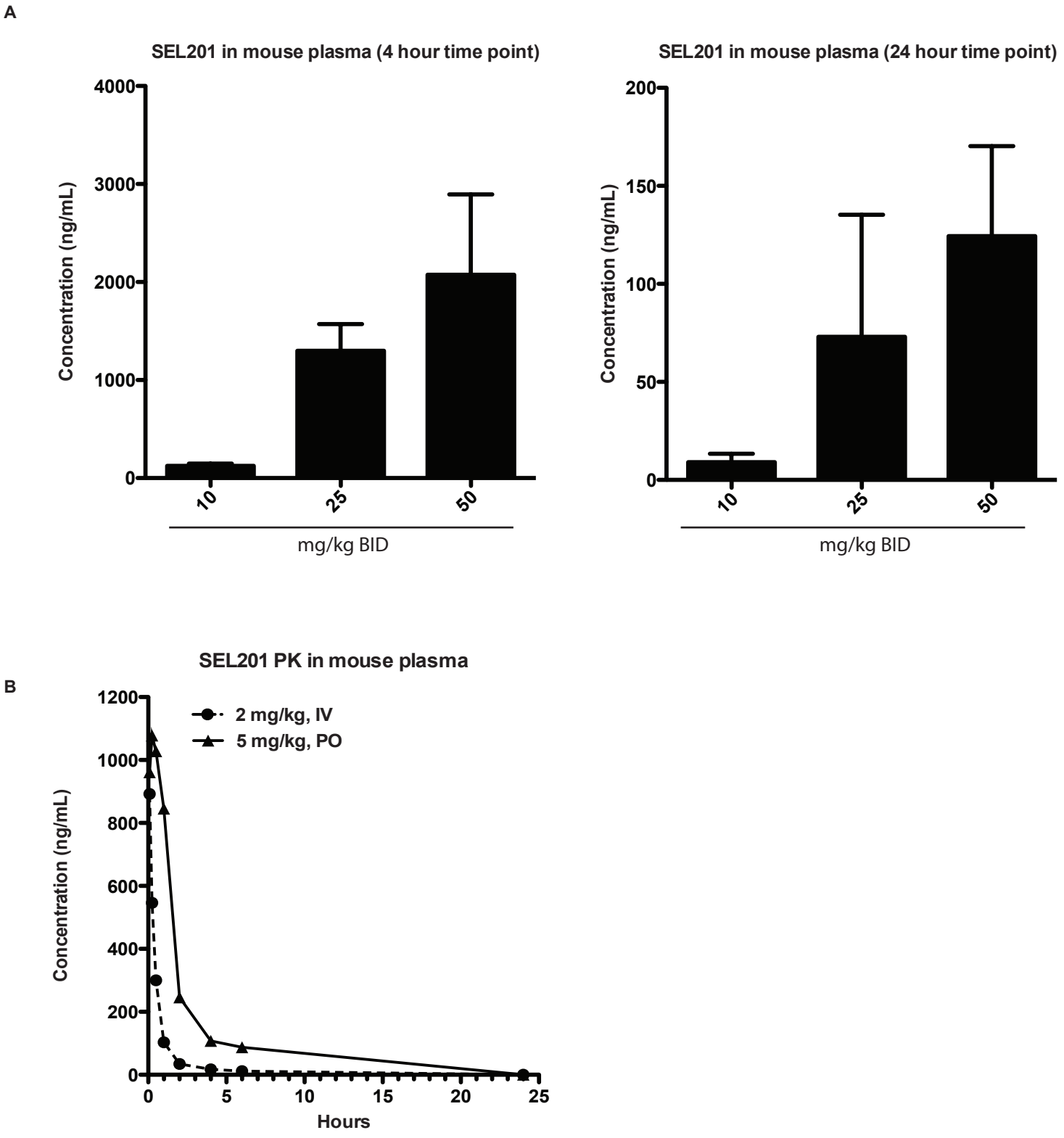

Supplementary Figure S4. Pharmacokinetic properties of SEL201 in mice.
(A) Pharmacodynamic properties of SEL201 at the doses of 10, 25 and 50 mg/kg BID (i.e. equivalents of 20, 50 and 100 mg/kg/day) were determined in mice (six animals per group). After a total of five oral administrations, three animals per 4h and 24h time point were sacrificed. Plasma concentration of SEL201 (mean ± SD) was determined. (B) Pharmacokinetic profile of SEL201 in mice (three animals per each of eight time points) was determined after oral and intravenous administration. PO – per os, IV – intravenous.

Supplementary Figure S5

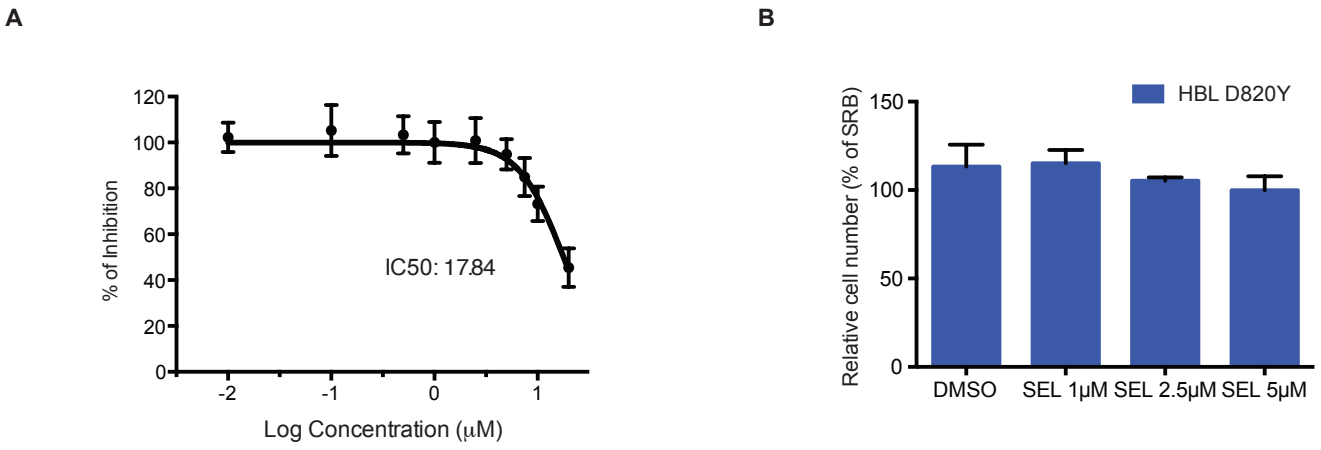

Supplementary Figure S5. Assessment of the efficacy of SEL201 in melanocytes and melanoma cells.
(A) Cell proliferation assessed by SRB staining after 72 hours with vehicle (DMSO) or SEL201 in MelST. IC50 was determined using Prism version 4.0 (GraphPad Software, San Diego, CA). (B) Cell proliferation assessed by SRB staining after 72 hours with vehicle (DMSO) or SEL201 in HBL cells. Data represent the mean ± SD, n=3. $p>0.05$, by One-way ANOVA.

Supplementary Figure S6

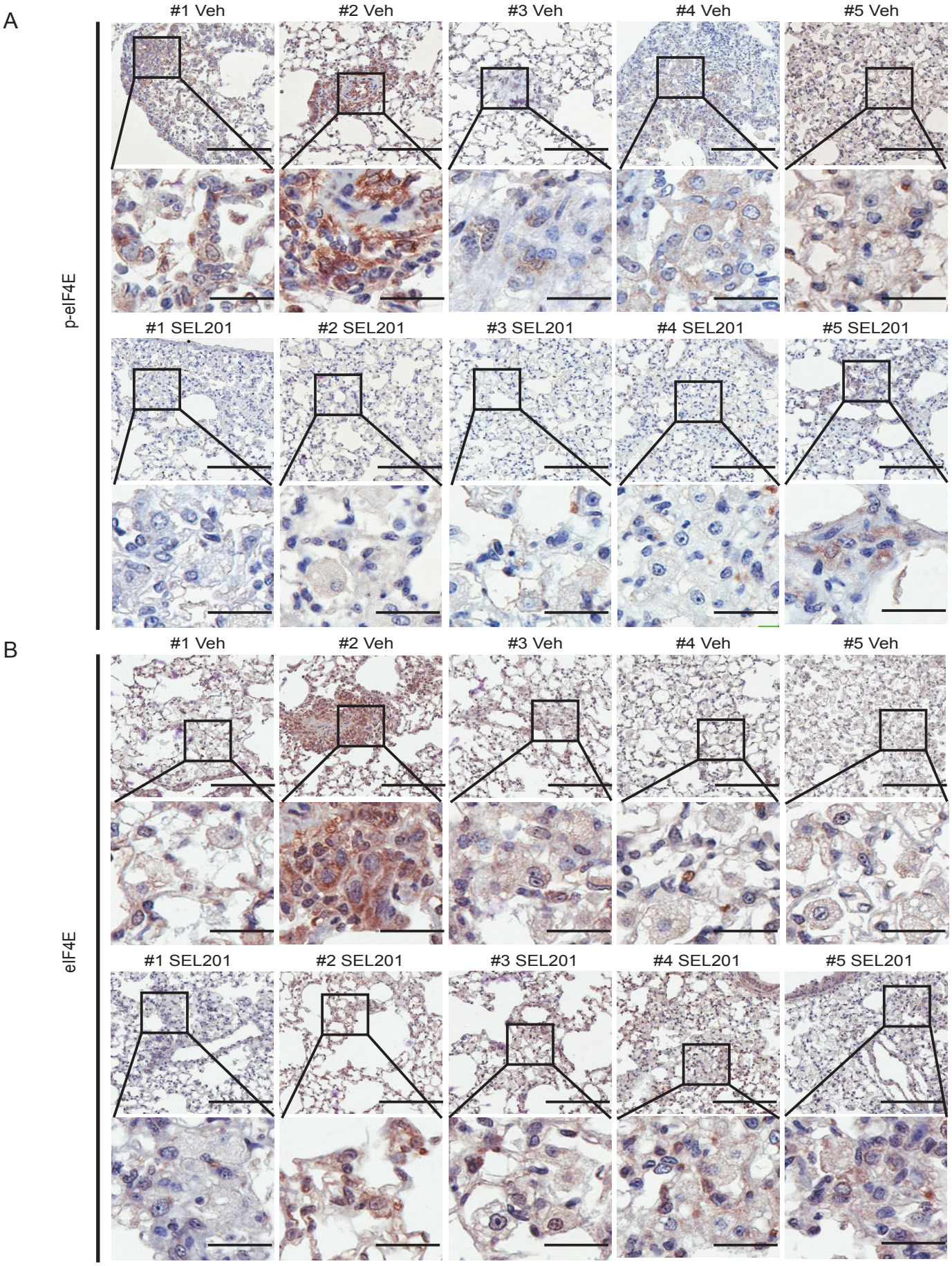

Supplementary Figure S6. Phosphorylation state of eIF4E in the lungs of tumor bearing SEL201 treated mice.
Representative images showing DAB staining for (A) phospho-eIF4E and (B) eIF4E in the tumors that developed in the lungs of mice described in Figure 6D. For upper panels in Vehicle (Veh) and SEL201 group, scale bars: 200 μm, original magnification: x4. For lower panels in Vehicle (Veh) and SEL201 group, scale bars: 40 μm, original magnification: x20.

Supplementary Table S1 Clinical information, including age, sex, thickness (Breslow), ulceration (The scores of phospho-eIF4E, phospho-MNK1 and MNK1 IHC staining are provided.)

Patient	C-KIT status	Subtype	Gender	Age	Thickness(mm)	Ulceration	p-MNK1(N/C)	p-eIF4E(N/C)	MNK1(N/C)
1	C-KIT WT	Acral	Female	27	2.5	No	2(+/+)	2(+/+)	1(+/+)
2	C-KIT WT	Mucosal	Female	52	-	-	3(-/+)	2(-/+)	3(-/+)
3	C-KIT WT	Acral	Female	65	8	No	1(-/+)	2(+/+)	1(-/+)
4	C-KIT WT	Acral	Male	41	8	Yes	0(-/-)	2(+/+)	1(+/+)
5	C-KIT WT	Acral	Male	59	5	Yes	1(-/+)	1(-/+)	0(-/+)
6	C-KIT WT	CSD	Male	66	6	Yes	0(-/-)	1(-/+)	1(+/+)
7	C-KIT WT	CSD	Female	42	3.9	-	0(-/-)	1(-/+)	1(-/+)
8	C-KIT WT	Acral	Male	45	1.3	No	2(-/+)	0(-/-)	1(-/+)
9	C-KIT WT	Acral	Male	44	5	Yes	0(-/-)	1(-/+)	1(-/+)
10	C-KIT WT	Acral	Female	61	3	Yes	0(-/-)	1(-/+)	0(-/-)
11	C-KIT WT	Mucosal	Male	65	7	No	1(+/+)	2(+/+)	1(+/+)
12	C-KIT WT	Mucosal	Female	26	-	Yes	1(-/+)	1(-/+)	0(-/-)
13	C-KIT WT	Mucosal	Female	45	-	-	2(+/+)	3(-/+)	2(+/+)
14	C-KIT WT	Mucosal	Female	35	8	Yes	1(+/-)	2(+/+)	3(+/+)
15	C-KIT K642E	Acral	Female	61	3	Yes	1(-/+)	2(-/+)	0(-/-)
16	C-KIT L576P	Acral	Female	57	2	No	1(-/+)	2(-/+)	2(-/+)
17	C-KIT L576P	Mucosal	Female	56	2	Yes	2(+/+)	3(-/+)	2(+/+)
18	C-KIT L576P	Mucosal	Male	51	5	Yes	0(-/-)	1(-/+)	0(-/-)
19	C-KIT L576P	Acral	Male	64	2.2	No	2(+/+)	2(-/+)	2(+/-)
20	C-KIT K642E	Acral	Male	62	4	Yes	2(+/+)	3(-/+)	2(+/+)
21	C-KIT L576P	Mucosal	Male	56	3	Yes	2(+/+)	3(-/+)	0(-/-)
22	C-KIT L576P	CSD	Male	66	3	No	3(-/+)	3(-/+)	2(-/+)
23	C-KIT L576P	CSD	Male	71	3.1	Yes	2(+/+)	3(-/+)	2(+/+)
24	C-KIT L576P	Mucosal	Male	63	-	No	2(+/+)	3(+/+)	2(+/+)

Supplementary Table S2 Pharmacokinetic properties of SEL201

A Pharmacokinetic profile of SEL201 in female mice (three animals per each of eight time points) was determined after oral and intravenous administration. PO – per os, IV – intravenous, T1/2 – elimination half-life, Cmax – peak plasma concentration, Tmax – time to reach Cmax, AUC – area under the curve, F – bioavailability

	Dose (mg/kg)	$T_{1/2}$ (h)	C_{max} (ng/mL)	T_{max} (h)	AUC_{0-t} (h*ng/mL)	F (%)
PO	5	1.44	1078	0.25	2035	~100%
IV	2	0.42	893	0.08	480	-

B Assessment of blood biochemistry in mice (three animals per group) administered with SEL201 at the dose of 50 mg/kg BID (100 mg/kg/day) was performed at the study termination on day 37. UREA – blood urea nitrogen, CREA – Creatinine, CK – Creatine kinase, TP- total protein, ALB – Albumin, CHOL – cholesterol, TGC – triglycerides; Na – sodium ions, K – potassium ions, Ca – calcium ions, Cl – chloride ions.

	UREA mmol/L	CREA mg/dL	CK U/L	TP g/dL	ALB g/dL	CHOL Mg/dL	TGC Mg/dL	Na mmol/L	K mmol/L	Ca mmol/L	Cl mmol/L
Control, Vehicle, BID	6.3	0.64	2519	3.6	3.4	129	307	124	2.9	2.2	67
SEL201, 50mg/kg, BID	6.7	1.79	2738	4.8	3.9	164	308	131	3.4	2.1	68

C Assessment of total blood cell counts in mice (three animals per group) administered with SEL201 at the dose of 50 mg/kg BID (100 mg/kg/day) was performed at the study termination on day 37. RBC – red blood cells, HGB – hemoglobin, HCT – hematocrit; MCV – mean corpuscular volume, MCH - mean corpuscular hemoglobin, MCHC - mean corpuscular hemoglobin concentration, RDW – red cell distribution width; WBC – white blood cells, LYMPH – lymphocytes, MONO – monocytes, GRA – granulocytes, PLT – platelet, MPV – mean platelet volume.

	RBC $10^6/mm^3$	HGB g/dL	HCT %	MCV μm^3	MCH pg	MCHC g/dL	RDW %	WBC $10^3/mm^3$	LYMPH %	MONO %	GRA %	PLT $10^3/mm^3$	MPV μm^3
Control, Vehicle, BID	8.6	13.1	43.6	50.7	15.3	30	11.7	4.4	63.7	6.3	30	836	5.1
SEL201, 50mg/kg, BID	8.1	11.6	39.7	49.3	14.4	29.4	12.2	6.3	56.7	6.9	36.4	487	5.6